AUT Journal of Mechanical Engineering

AUT J. Mech. Eng., 8(2) (2024) 123-134
DOI: 10.22060/ajme.2024.22965.6089

Optimum design of a viscoelastic vibration absorber for counter-rotating systems

Mohammad Omidpanah*

Department of Mechanical Engineering, National University of Skills (NUS), Tehran, Iran

ABSTRACT: The small distance between two rotating shafts can disturb them, cause interference in their performance, and affect the system's efficiency. The application of the counter-rotating double shafts has some specific benefits. For example, these shafts can be used under the water to neutralize the driving torque effect, prevent the submarine's self-propulsion, and increase the submarine's power to move forward and maneuver. The aim of this study is designing an optimum viscoelastic vibration absorber for a Counter-Rotating Double Shaft to deal with the vibration. In order to overcome vibrations, Viscoelastic cylinders are modeled as distributed spring and damper which are considered between the two shafts, and their vibration equations are obtained. Optimal position and distributed stiffness and damping coefficients are determined using a particle swarm optimization algorithm. The objective function to be minimized is defined as the relative distance between shafts which is controlled by Equivalent stiffness and damping coefficients of considered viscoelastic vibration absorber. The present results show that applied viscoelastic polymer with the nearest features to the optimum values can drastically decrease the relative distance between shafts and absorb the vibration of rotating shafts.

Review History:

Received: Feb. 16, 2024
Revised: May, 19, 2024
Accepted: Jul. 17, 2024
Available Online: Jul. 27, 2024

Keywords:

Counter-Rotating Double Shaft
Vibration Absorber
Viscoelastic Materials
PSO Optimization

1- Introduction

The application of the counter-rotating double shafts has some specific benefits. For example, these shafts can be used under the water to neutralize the driving torque effect, prevent the submarine's self-propulsion, and increase the submarine's power to move forward and maneuver. The cavitation and noise problem of these counter-rotating double shafts can also be addressed by designing propellers with smaller diameters. In the case that one of the motors connected to shafts is incapacitated, the submarine can still move forward under the water. However, the rotating movements of the shafts can intensify the vibrations, which cause disturbance. Furthermore, the little distance between shafts increases the possibility of their contact with each other, which consequently disturbs the system's performance. To prevent interference between shafts, their vibrations should be controlled.

To the best of our knowledge, no study has ever considered vibrations of the counter-rotating double shafts in the presence of vibration absorber material between rotating shafts.

Since the most important practical application of the present study is about lubrication of Coaxial rotating shafts which are charged with a polymeric viscoelastic material such as industrial oil or grease. Sarath et al. [1] have Reviewed the tribological behavior of polymeric materials. The optimal design of viscoelastic vibration absorbers for rotating systems was studied by Doubrawa Filho [2]. Jin et al. [3] have studied the complex vibrational behavior of dual rotor aero engine by FEM and the dynamic stability of their model was compared with measurements. Wong et al. [4] using modified fixed-points theory designed an optimization of a viscoelastic dynamic vibration absorber. The design of optimum viscoelastic vibration absorbers based on the fractional calculus model was studied by Spindola [5] and Numerical examples are produced and discussed.

The free vibration analysis of a nonlinear slender rotating shaft with simply support conditions was studied by Shahgholi et al. [6]. Since the effect of shear deformation was negligible in the slender rotating shaft, the researchers modeled a system rotary inertia and studied the gyroscopic effect. The equations of motion were derived using the extended Hamilton principle and the nonlinear system was analyzed utilizing the multiple scales method. The forward and backward nonlinear frequencies of the slender rotating shaft were obtained. The scholars concluded that to have the natural vibration of a slender rotating shaft, backward and forward modes were required. In the same vein, Hosseini and Khadem [7] investigated the free vibrations of an in-extensional simply supported rotating shaft with nonlinear curvature and inertia. Although the rotary inertia and gyroscopic effects were included, the shear deformation was neglected. They applied the multiple scales method to analyze the free vibrations of the shaft. This method was

*Corresponding author's email: momidpanah@tvu.ac.ir

Fig. 1. Schematic of counter-rotating double shaft

Table 1. Dimensions of the counter-rotating double shaft

R_1	15.5 mm
R_2	22.5 mm
R_3	27.6 mm
R_4	35 mm
Length of outer shaft	1195 mm
Length of inner shaft	1300 mm
Relative distance between of two shafts	5.1 mm

applied to the discretized equations and directly to the partial differential equations of motion. Huang et al. [8] focused on the noise prediction of a rotating shaft. They applied Hamilton's principle and Galerkin's method to establish the motion governing equations for a Rayleigh beam that rotated about its longitudinal axis and was subjected to a harmonic force. The aim was to solve the vibrating displacement of the shaft. In this regard, the aeroacoustics theory, introduced by Lighthill and improved by Ffowcs Williams and Hawkings was used for calculating the developed noise of the shaft in motion.

Although some recent studies were conducted on vibrations of the rotating shafts, no research has ever designed a vibration absorber for controlling the vibrations of the counter-rotating double shafts and preventing contact between them. In this research, a distributed spring and damper were considered between the two shafts and the vibration equations of the shafts were obtained as a couple. Furthermore, the optimum placement and distributed damping and stiffness coefficient were obtained using the particle swarm optimization (PSO) algorithm. To design the vibration absorber between two shafts, viscoelastic materials have been used. Accordingly, in the first step, these materials have been modeled as a distributed spring and damper between two shafts. Next, the nearest polymer of viscoelastic materials with optimized features was considered as the vibration absorber. Finally, a polymer from a list of viscoelastic materials with the nearest features to the optimum distributed damper and spring has been chosen as the vibration absorber.

2- Vibration equations

In this study, two rotating shafts are considered as cylinders with the same rotational axis which rotate in opposite directions. The schematic of the model is shown in Fig.1 and their dimensions are brought in Table 1. Axial propulsion force, which is applied to the end of the shafts, and the rotating frequency of the inner and outer shafts are brought in Table 2.

A rotating shaft with axial applied force can be considered as a cantilever beam. The vibration equation of this shaft can be obtained using Eq. (1), [9].

Table 2. Propulsion force and rotating frequencies of the counter-rotating double shaft

F	ω_i	ω_o	$P_i\begin{pmatrix} axial\ force\ for \\ inner\ shaft \end{pmatrix}$	$P_o\begin{pmatrix} axial\ force\ for \\ outter\ shaft \end{pmatrix}$
2000N	1500rpm	1500rpm	4000N	4000N

$$EI\frac{\partial^4 w(x,t)}{\partial x^4}+P\frac{\partial^2 w(x,t)}{\partial x^2}+\rho A\frac{\partial^2 w(x,t)}{\partial t^2}=0 \qquad (1)$$

where,

E, ρ, A and P are shaft's Young's modulus, density, surface section, and axial force, respectively.

Rotating shaft angular velocity causes inertia force. So, the rotating shaft vibration equation can be expressed by Eq. (2).

$$EI\frac{\partial^4 w(x,t)}{\partial x^4}+P\frac{\partial^2 w(x,t)}{\partial x^2}+\rho A\frac{\partial^2 w(x,t)}{\partial t^2}=\rho A\Omega^2 w(x,t) \qquad (2)$$

Different disturbances such as force caused by unbalances, sea waves and water flow are applied to the shaft such as external forces. Since the shaft is rotating with the angular velocity of Ω it can be said that excitation force has the same frequency. In this study, it is assumed that a force (F) exists at the beginning part of the shaft and its vibration equation can be driven as Eq. (3).

$$\frac{EI}{\rho A}\frac{\partial^4 w(x,t)}{\partial x^4}+\frac{P}{\rho A}\frac{\partial^2 w(x,t)}{\partial x^2}-\Omega^2 w(x,t)+\frac{\partial^2 w(x,t)}{\partial t^2}=F\sin\Omega t\,\delta(x-L_0) \qquad (3)$$

By employing the assumed mode method vibration equation can be rewritten as Eq. (4).

$$\sum_{n=1}^{\infty}\left[\left(EI\frac{d^4 W_n}{dx^4}+P\frac{d^2 W_n}{dx^2}-\rho A\Omega^2 W_n\right)\eta_n(t)+\rho A W_n\ddot{\eta}_n(t)\right]=0 \qquad (4)$$

where, W_n is the mode of a cantilever beam. After multiplying each side of the equation by W_s and performing integration along the shaft length, the vibration equation can be written as Eq. (5).

$$\left(\rho A_o\int_0^l W_{o_s}W_{o_s}dx\right)\ddot{\eta}_s(t)+\sum_{m=1}^{2}\left[\left(\int_0^l\left(EI_o\frac{d^4 W_{o_m}}{dx^4}+P_o\frac{d^2 W_{o_m}}{dx^2}-\rho A_o\Omega_o{}^2 W_{o_m}\right)W_{i_s}dx\right)\eta_m(t)\right]=\int_0^l F\sin\omega t\,\delta(x-L_o)W_{o_s}dx \qquad (5)$$

After solving Eq. (5) using the Runge–Kutta method, the time function η_n can be extracted. Considering this time function, vibrations of the external shaft with harmonic excitations will be obtained.

As it can be seen in Fig.2, vibrations exceeded 5.1mm range and the two shafts have contact with each other.

3- Verification

Based on the shaft's equations of motion, we compared our findings with the results of a similar study. Tavari et al. [9] examined a shaft affected by an external load (cutting tool). The workpiece shaft was modeled as a cantilever beam and its equations of motion were obtained in three directions (two directions in the surface section of the shaft and one direction in the twisted movement of the shaft). To solve the system equations, we considered the initial conditions similar to the research by Tavari et al. [9]. The results were similar as Fig.3 shows.

It is seen that the values obtained by the present work have very well agreement by ref Tavari et al [9].

4- Vibration absorber design

As discussed previously, the contact between the two shafts should be controlled to avoid system disturbance. Therefore, a vibration absorber was used between the two shafts. In this case, the vibration equations of the internal and

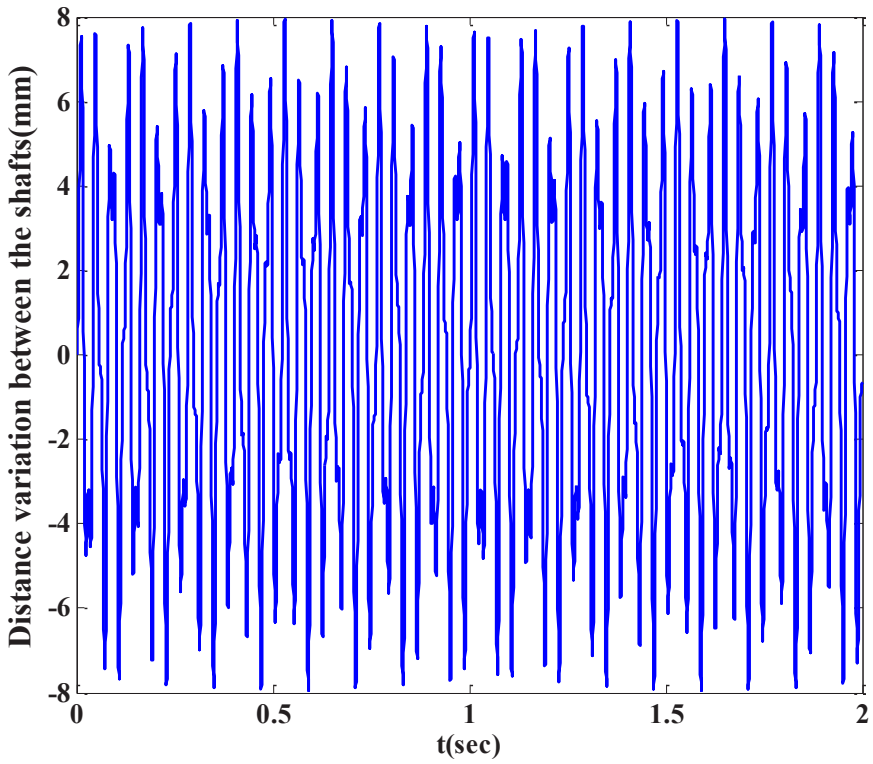

Fig. 2. Distance variation between the shafts

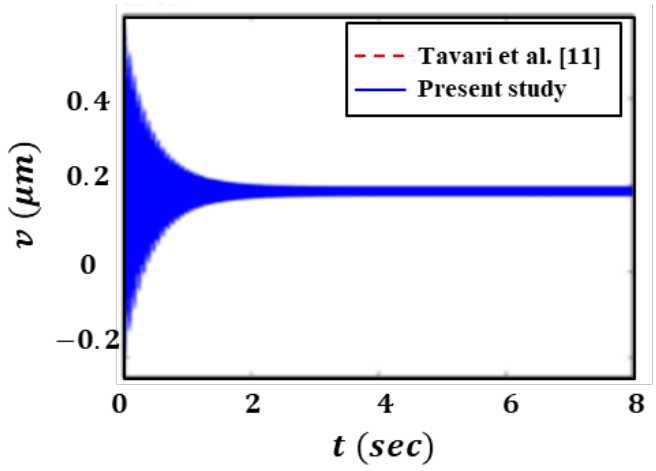

Fig. 3. Transverse vibration response by considering similar initial conditions to Tavari et al. research [9].

Table 3. Comparing Elastic displacement in the y direction with respect to the time of this study and ref [10]

	Elastic displacement in the y direction	
Time (Sec)	Present Study	Ref [10]
0.0936	0.498	0.497
0.14	0.445	0.445
0.257	0.398	0.398
0.327	0.364	0.363
0.398	0.336	0.338
0.468	0.308	0.309
0.538	0.287	0.288
0.63	0.268	0.268
0.772	0.240	0.241
0.912	0.225	0.225
1.10	0.206	0.207
1.29	0.194	0.196
1.52	0.188	0.187
1.82	0.182	0.183
2.27	0.179	0.176
0.302	0.176	0.174
0.430	0.180	0.179
0.737	0.181	0.180

external shafts were coupled with each other by the stiffness and damping coefficients of the absorbing material. Vibration equations of shafts can be rewritten using assumed modes methods within the time domain [10].

$$\begin{aligned}&\frac{E_i I_i}{\rho_i A_i}\frac{\partial^4 w_i(x,t)}{\partial x^4}+\frac{P_i}{\rho_i A_i}\frac{\partial^2 w_i(x,t)}{\partial x^2}\\&-\Omega_i{}^2 w_i(x,t)+\frac{\partial^2 w_i(x,t)}{\partial t^2}=\\&(k_{eq}(w_o(x,t)-w_i(x,t))\\&+c_{eq}(\dot{w}_o(x,t)-\dot{w}_i(x,t)))\\&\times\left(u\left(x-a+\frac{b}{2}\right)-u\left(x-a-\frac{b}{2}\right)\right)\end{aligned}\tag{6}$$

$$\begin{aligned}&\frac{E_o I_o}{\rho_o A_o}\frac{\partial^4 w_o(x,t)}{\partial x^4}+\frac{P_o}{\rho_o A_o}\frac{\partial^2 w_i(x,t)}{\partial x^2}\\&-\Omega_o{}^2 w_o(x,t)+\frac{\partial^2 w_o(x,t)}{\partial t^2}=\\&(k_{eq}(w_i(x,t)-w_o(x,t))\\&+c_{eq}(\dot{w}_i(x,t)-\dot{w}_o(x,t)))\\&\left(u\left(x-a+\frac{b}{2}\right)-u\left(x-a-\frac{b}{2}\right)\right)\\&+F\sin\omega t\,\delta(x-L_o)\end{aligned}\tag{6}$$

Using the assumed modes method and considering modes of the cantilever beam, Eqs. (6) can be rewritten as Eqs. (7).

$$\left(\rho A_i \int_0^l W_{i_s} W_{i_s} dx\right) \ddot{\eta}_s(t) + \sum_{n=1}^{2}\left[\left(\int_0^l \left(c_{eq} g(x) W_{in}\right) W_{i_s} dx\right) \dot{\eta}_n(t)\right] + \sum_{n=1}^{2}\left[\left(\int_0^l \begin{pmatrix} EI_i \frac{d^4 W_{in}}{dx^4} + P_i \frac{d^2 W_{in}}{dx^2} \\ -\rho A_i \Omega_i^2 W_{in} + k_{eq} g(x) W_{in} \end{pmatrix}_n W_{i_s} dx\right) \eta_n(t)\right] - \sum_{m=1}^{2}\left[\left(\int_0^l \left(c_{eq} g(x) W_{o_m}\right) W_{i_s} dx\right) \dot{\eta}_m(t)\right] - \sum_{m=1}^{2}\left[\left(\int_0^l \left(k_{eq} g(x) W_{om}\right) W_{i_s} dx\right) \eta_m(t)\right] = 0$$

$$\left(\rho A_o \int_0^l W_{o_s} W_{o_s} dx\right) \ddot{\eta}_s(t) + \sum_{m=1}^{2}\left[\left(\int_0^l \left(c_{eq} g(x) W_{om}\right) W_{o_s} dx\right) \dot{\eta}_m(t)\right] + \sum_{m=1}^{2}\left[\left(\int_0^l \begin{pmatrix} EI_o \frac{d^4 W_{om}}{dx^4} + P_o \frac{d^2 W_{om}}{dx^2} \\ -\rho A_o \Omega_o^2 W_{om} + k_{eq} g(x) W_{om} \end{pmatrix} W_{i_s} dx\right) \eta_m(t)\right] - \sum_{n=1}^{2}\left[\left(\int_0^l \left(c_{eq} g(x) W_{in}\right) W_{o_s} dx\right) \dot{\eta}_n(t)\right] - \sum_{n=1}^{2}\left[\left(\int_0^l \left(k_{eq} g(x) W_{in}\right) W_{o_s} dx\right) \eta_n(t)\right] = \int_0^l F \sin\omega t\, \delta(x - L_o) W_{o_s} dx = F W_{o_s}(L_0) \sin\omega t \tag{7}$$

where,

$$g(x) = u\left(x - a + \frac{b}{2}\right) - u\left(x - a - \frac{b}{2}\right) \tag{8}$$

In Eq. (8), it is assumed that the absorbing material with a length b that is considered 5cm to exist between two shafts. Furthermore, the parameter a is the position of the absorbing material that will be obtained by optimization methods.

5- Position and features determination of optimized absorber with PSO algorithm

The position and features of the vibration absorber are effective parameters on system vibration. Therefore, $a, k, c,$, that are the position, stiffness, and damping coefficient of the absorber were considered as the optimization parameters.

In this paper, in order to achieve the optimum values of a, k, c, Particle Swarm Optimization (PSO) was considered as the optimization algorithm. Among the available optimization algorithms, PSO algorithm has been used in many studies due to its specific features. Since this research aimed to prevent contact between shafts, the cost function was considered the sum of the absolute value of the distance variation between the two shafts in a specific time interval. It should be noted that in this optimization, the searching range for k and c was considered $[0, 5000000]$ and Table 4 shows configurations of the PSO algorithm. Optimum values of parameters a, k, c, have been achieved and brought in Table 5.

6- Determination of vibration absorber material

In mechanical systems, vibration and noise can be controlled or decreased using several approaches. In recent years, viscoelastic materials have been considered as one

Table 4. PSO algorithm settings

Population Size	Personal Learning Coefficient	Global Learning Coefficient	Inertia Weight	Inertia Weight Damping Ratio
100	30000	50000	1	0.98

Table 5. Optimized values for parameters a, c and k

	a	*c*	*k*	*fittness*
Best Solution	1.175	1.59*e*5	4.21*e*6	0.1944

Table 6. Specifications of polymers

Polymer	G_0 (MPa)	G_∞ (GPa)	τ_s	α	β	*Density* (g/cm^3)	T_g (^{o}C)	Ref.
1	2.144	1.859	1.649E-7	0.5709	0.0363	1.074	-40	[12]
2	1.558	3.573	1.574E-6	0.5332	0.0269	1.092	-21	[12]
3	2.340	2.375	1.757E-3	0.6174	0.0259	1.108	2	[12]
4	2.370	1.169	7.974E-4	0.6138	0.0695	1.123	6	[12]
5	1.490	1.415	2.991E-4	0.6608	0.0533	1.073	2	[12]
6	1.917	2.395	1.598E-7	0.5555	0.0309	1.072	-39	[12]
7	2.002	2.129	1.468E-4	0.6378	0.0296	1.084	0	[12]
8	2.307	1.099	2.974E-3	0.6797	0.0566	1.119	9	[12]
9	1.762	1.626	9.576E-8	0.5343	0.0659	1.060	-35	[12]
10	2.243	0.8208	3.107E-3	0.7236	0.0935	1.106	11	[12]
11	2.312	1.032	2.971E-7	0.6396	0.0733	1.064	-34	[12]
12	1.634	2.156	7.127E-8	0.4998	0.0460	1.087	-43	[13]
13	1.857	1.107	1.214E-8	0.5347	0.1310	1.073	-51	[13]
14	6.388	0.9417	3.319E-7	0.5480	0.1066	1.090	-35	[14]
15	6.100	0.8674	3.493E-8	0.5280	0.1323	1.079	-42	[14]
16	1.728	1.888	8.268E-2	0.6602	0.0574	1.170	28	[15]
17	5.578	1.021	1.178E-4	0.5558	0.2108	1.154	-6	[15]
18	3.372	1.453	3.139E-9	0.4833	0.4116	1.101	-36	[15]
19	5.019	0.8089	1.702E-1	0.4941	0.1356	1.096	13	[16]
20	12.71	1.678	7.764E-9	0.2609	0.1973	1.139	-48	[12]
21	11.01	1.055	4.92E-11	0.2947	0.3779	1.105	-57	[12]

of the common and low-cost approaches. In this study, a viscoelastic material with both elastic and viscosity characteristics has been used; in other words, the selected material has two features; damping property (Energy loss) and structural property (Energy saving). These kinds of polymers are known as passive dampers. Dynamic features of these materials under harmonic excitation can be expressed by complex elasticity modulus $\left(\sigma(t)/\varepsilon(t)=E'+iE''\right)$, which is due to the phase time difference between the strain and stress. To control the vibration of the system, polymers from different studies [10-14] have been used as a damping middle layer. Their operations in the system have been compared to each other to find a suitable absorber, that has the nearest stiffness and damping coefficients to the optimum values. Polymer characteristics are shown in Table 6.

Curve fitting parameters of each polymer are brought in Hartmann et al. [15]. Also, in this research curve fitting process and all required parameters were introduced. Considering the HN model represented in [16]. The elasticity modulus and damping coefficient of the polymers can be obtained with appropriate accuracy in a wide range of frequencies.

In order to consider the effect of vibration absorber material in the equations, an equivalent stiffness and damping coefficient of the absorber should be entered in the equations. To clarify this matter, one shaft was considered under axial load, and the equivalent spring was obtained.

$$\delta=\frac{FL}{EA}=\frac{F}{K}\quad\rightarrow\quad K_{eq}=\frac{EA}{L} \tag{9}$$

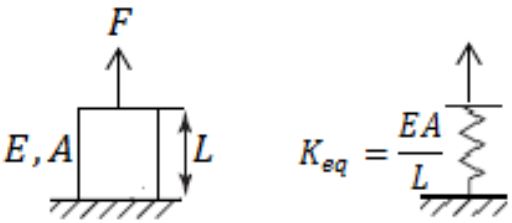

Fig. 4. Model of equivalent spring

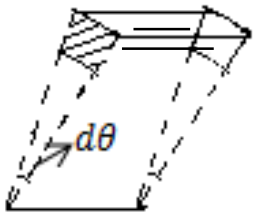

Fig. 6. Vibration absorber element

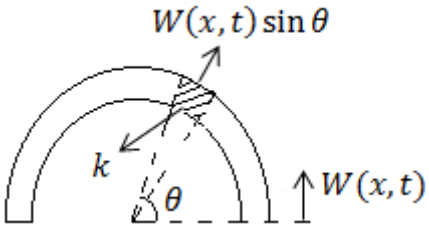

Fig. 5. Vibration absorber modeling

Since the absorber was used in a small range of shaft length, the dominant vibration mode in the absorber was equal to the vibrations along the shell thickness, and bending effects were neglected. On the other hand, according to slippage between shafts and absorber, it is obvious that the absorber is just under the pressure. So, half of the cylindrical absorber is always under the pressure.

In order to achieve the distributed stiffness coefficient of the vibration absorber in shaft length, the stiffness coefficient of the element should be initially calculated. It also should be noted that due to the absorber thickness smaller than its diameter, an approximately rectangular shape can be considered for the element.

$$k = \frac{EA}{L} = \frac{E(rd\theta dx)}{d} \tag{10}$$

Later, the energy method was used and the stiffness coefficient of the equivalent absorber was calculated as Eq. (11).

$$\frac{1}{2}k_{eq}W^2 = \int_0^{\pi}\frac{1}{2}\frac{E(rdx)}{d}W^2(\sin\theta)^2 d\theta = \frac{\pi}{4}\frac{E(rdx)}{d}W^2 \tag{11}$$

$$k_{eq} = \frac{\pi}{2}\frac{E(rdx)}{d}$$

where, d and r are the thickness and average diameter of the absorber, respectively. As it was described in previous sections, in viscoelastic materials, Young's modulus can be replaced as a complex number in the equations. Furthermore, the method mentioned in De Silva's book [17] can also be used in Eq. (12).

$$E^* = E' + \left(\frac{E''}{\omega}\right)\frac{\partial}{\partial t} \tag{12}$$

Considering these explanations, the equivalent distributed stiffness and damping coefficient of the absorber in the longitudinal direction of the shaft is written in Eqs. (13).

$$k_{eq} = \frac{\pi}{2}\frac{rE'}{d}$$
$$c_{eq} = \frac{\pi}{2}\frac{rE''}{\omega d} \tag{13}$$

It should be noted that temperature and frequency have some specific effects on viscoelastic materials. So, the applied forces should be determined initially. Since noise on the motor shafts has a motor frequency, a harmonic force can be assumed with the frequency of ω (shaft frequency) at the head of the external shaft.

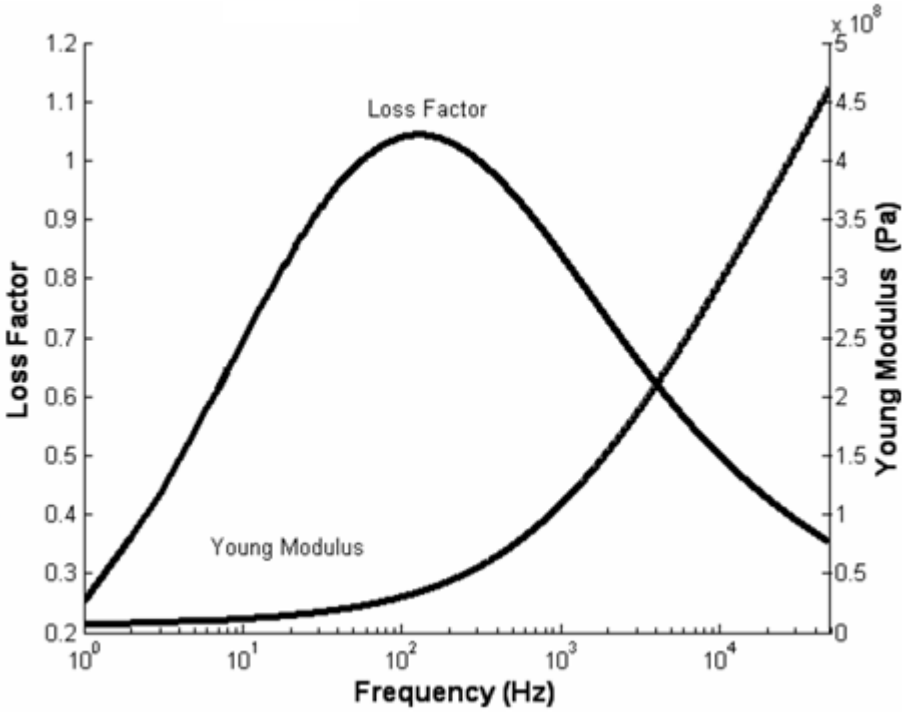

Fig. 7. Young's modulus and damping coefficient of polymer number 7

$$f(x,t) = F\sin\omega t\,\delta(x - L_o) \tag{14}$$

Using the given ω, equivalent stiffness and damping coefficients of the absorber can be obtained for each polymer and the polymer with the nearest coefficients to the optimum values can be selected. Results show that stiffness coefficient variations have no effects on the system response because the total stiffness coefficient of the structure is more significant than the absorber coefficient. Therefore, the main parameter to select the material is the equivalent damping coefficient. Comparison between the damping coefficients of different polymers shows that type 7 has the nearest equivalent damping coefficient to the optimum value. Using the Young's modulus and loss factor in shaft frequency, the damping coefficient can be obtained for each polymer by Eq. (13). The damping coefficient of polymer 7 is $1.3838e5$, which is the nearest to the optimum value.

By replacing the equivalent stiffness and damping coefficient of the designed absorber in the vibration equations and solving these equations as a couple to each other, the system response can be achieved. Fig.8 shows the distance variations between the two shafts.

With regard to Fig.8, it can be concluded that the relative distance between the two shafts was controlled appropriately and their contact was prevented.

7- Conclusion

Using two counter uniaxial shafts in ships and submarines with pre-drive systems can increase the maneuvers of their motors. However, it should be considered that movements due to vibration of the rotating shafts can cause contact between them and lead to disturbance in system operation. So, it is important to control the vibrations of the double counter shafts. The proposed method in this study was based on the application of viscoelastic materials. These materials have been used between two shafts and vibration equations of these shafts have been extracted as a couple with each other. PSO algorithm has been employed to obtain the optimum position and features of the vibration absorber. According to the proposed model for the viscoelastic cylinder, an appropriate viscoelastic polymer has been selected.

Variations in relative distance between shafts show that the designed absorber can control the distance appropriately and prevent contact between two shafts. The distance between the inner and outer shafts was 5.1mm. During system operation without a vibration absorber maximum distance variation between the two shafts was $8mm$; so, contact between the shafts and disturbances in system operation was observed.

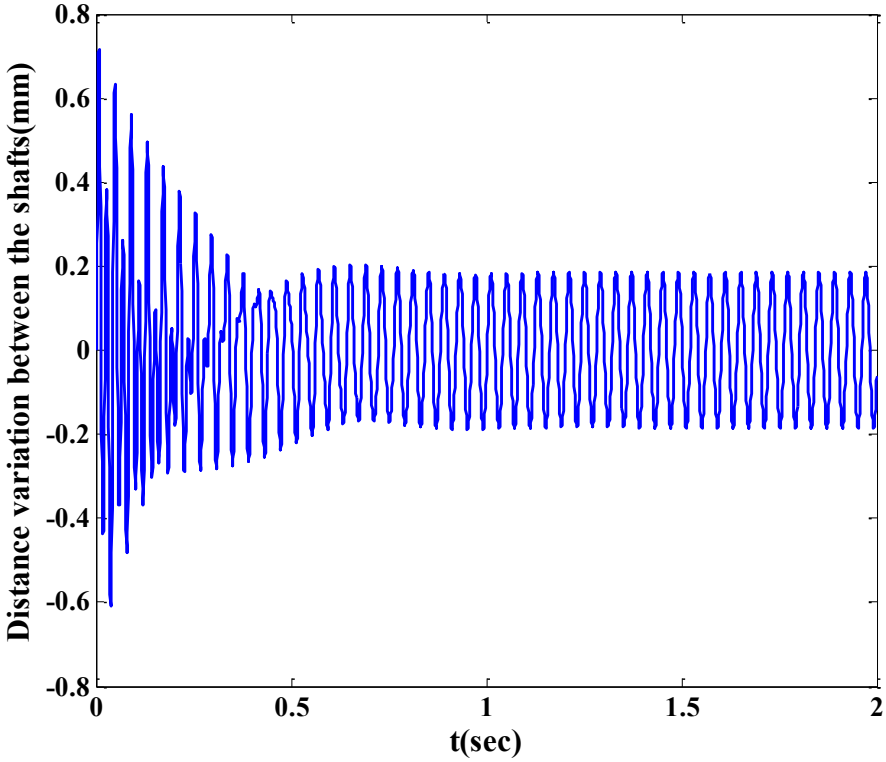

Fig. 8. Distance variation between two shafts after using the vibration absorber

However, after using the vibration absorber in the considered position, it was observed that the maximum distance variation was reduced to 0.2mm.

References

[1] P. Sarath, R. Reghunath, J.T. Haponiuk, S. Thomas, S.C. George, Introduction: A journey to the tribological behavior of polymeric materials, in: Tribology of Polymers, Polymer Composites, and Polymer Nanocomposites, Elsevier, 2023, pp. 1-16.

[2] F. Doubrawa Filho, M. Luersen, C. Bavastri, Optimal design of viscoelastic vibration absorbers for rotating systems, Journal of Vibration and Control, 17(5) (2011) 699-710.

[3] Y. Jin, X. Zhou, X. Quan, X. Zhang, K. Lu, J. Wang, Topological structures of vibration responses for dual-rotor aeroengine, Mechanical Systems and Signal Processing, 208 (2024) 111053.

[4] W.O. Wong, R. Fan, F. Cheng, Design optimization of a viscoelastic dynamic vibration absorber using a modified fixed-points theory, The Journal of the Acoustical Society of America, 143(2) (2018) 1064-1075.

[5] J. Espíndola, G. Cruz, E. Lopes, C. Bavastri, Design of optimum viscoelastic vibration absorbers based on the fractional calculus model, Proceedings of the XI DINAME, Ouro Preto-MG–Brazil, (2005).

[6] M. Shahgholi, S. Khadem, S. Bab, Free vibration analysis of a nonlinear slender rotating shaft with simply support conditions, Mechanism and Machine Theory, 82 (2014) 128-140.

[7] S. Hosseini, S. Khadem, Free vibrations analysis of a rotating shaft with nonlinearities in curvature and inertia, Mechanism and Machine theory, 44(1) (2009) 272-288.

[8] Y. Huang, T. Chen, P. Shieh, Analytical estimation of the noise due to a rotating shaft, Applied acoustics, 76 (2014) 187-196.

[9] H. Tavari, M.M. Jalili, M.R. Movahhedy, Nonlinear analysis of chatter in turning process using dimensionless groups, Journal of the Brazilian Society of Mechanical Sciences and Engineering, 37 (2015) 1151-1162.

[10] B. Hartmann, J.V. Duffy, G.F. Lee, E. Balizer, Thermal

and dynamic mechanical properties of polyurethaneureas, Journal of applied polymer science, 35(7) (1988) 1829-1852.

[11] J.V. Duffy, G.F. Lee, J.D. Lee, B. Hartmann, Dynamic Mechanical Properties of Poly (tetramethylene ether) Glycol Polyurethanes: Effect of Diol-Chain Extender Structure, in, ACS Publications.

[12] D.J. Lee J.D., Hartmann B., Lee G., Thermal anD dynamic Mechanical Properties of Some TDI and MDI Based Polyurethane Areas, in: AIChE meeting [papers], American Institute of Chemical Engineers, New York, 1989, pp. 20.

[13] B. Hartmann, G.F. Lee, Dynamic mechanical relaxation in some polyurethanes, Journal of non-crystalline solids, 131 (1991) 887-890.

[14] J. Lee, G. Lee, B. Hartmann, Damping Properties of Aliphatic Polyurethanes from, 4, 4'Dicyclohexylmethane Diisocyanate, in: Proceeding of Damping, 1991.

[15] B. Hartmann, G.F. Lee, J.D. Lee, Loss factor height and width limits for polymer relaxations, The Journal of the Acoustical Society of America, 95(1) (1994) 226-233.

[16] S. Havriliak, S. Negami, A complex plane analysis of α-dispersions in some polymer systems, in: Journal of Polymer Science Part C: Polymer Symposia, Wiley Online Library, 1966, pp. 99-117.

[17] C.W. De Silva, Vibration damping, control, and design, Crc Press, 2007.

HOW TO CITE THIS ARTICLE

M. Omidpanah, Optimum design of a viscoelastic vibration absorber for counter-rotating systems, AUT J. Mech Eng., 8(2) (2024) 123-134.

DOI: 10.22060/ajme.2024.22965.6089